JIRRS
Journal International Review of Research Studies

Received: 19/09/2026 - **Accepted:** 26/10/2026
Vol: 01.07
DOI: 10.66104/p3c1fk38
Pages: 1-33

Alloy Nucleation, Coalescence, and Settling in Ni–Mo–V Smelting: A Critical Review

Antonio Clareti Pereira, PhD
PhD in Chemical Engineering
University of São Paulo (USP)
Belo Horizonte, Minas Gerais, Brazil
E-mail: claretipereira@gmail.com

https://orcid.org/0000-0001-8115-4279

Abstract

Recovering nickel, molybdenum, and vanadium from spent hydroprocessing catalysts by reductive smelting requires both chemical conversion and physical separation of alloy from slag. The latter is often simplified to equilibrium partitioning, although entrained droplets can remain unrecovered after reduction. This critical review evaluates metallic nucleation, alloy-droplet growth, interfacial forces, collision and coalescence, gravitational settling, slag rheology, and residence-time effects. Evidence is differentiated between direct Ni–Mo–V studies and transferable, but composition-dependent, findings from copper, steel, and matte–slag systems. We use Stokes settling only as a limiting reference and propose a mechanism-preserving measurement framework for scale-up. The synthesis indicates that chemical reduction, metal-droplet size distributions, viscosity, local flow, and interfacial conditions must be quantified together before recovery performance can be credibly extrapolated. The principal research gap is a coupled, independently validated metal–slag separation dataset for Ni–Mo–V catalyst-derived melts.

Keywords: spent hydroprocessing catalysts; Ni–Mo–V alloy; droplet coalescence; metal–slag interface; slag viscosity; gravitational settling

Highlights

Chemical reduction and physical capture are distinct controls on Ni–Mo–V recovery.
Droplet-size distributions and slag rheology jointly govern settling.
Copper and steel slag evidence is transferable only with explicit qualification.
Scale-up requires coupled droplet imaging, phase balances, and residence-time data.

JIRRS
Journal International Review of Research Studies

Received: 19/09/2026 - **Accepted:** 26/10/2026
Vol: 01.07
DOI: 10.66104/p3c1fk38
Pages: 1-33

Graphical Abstract

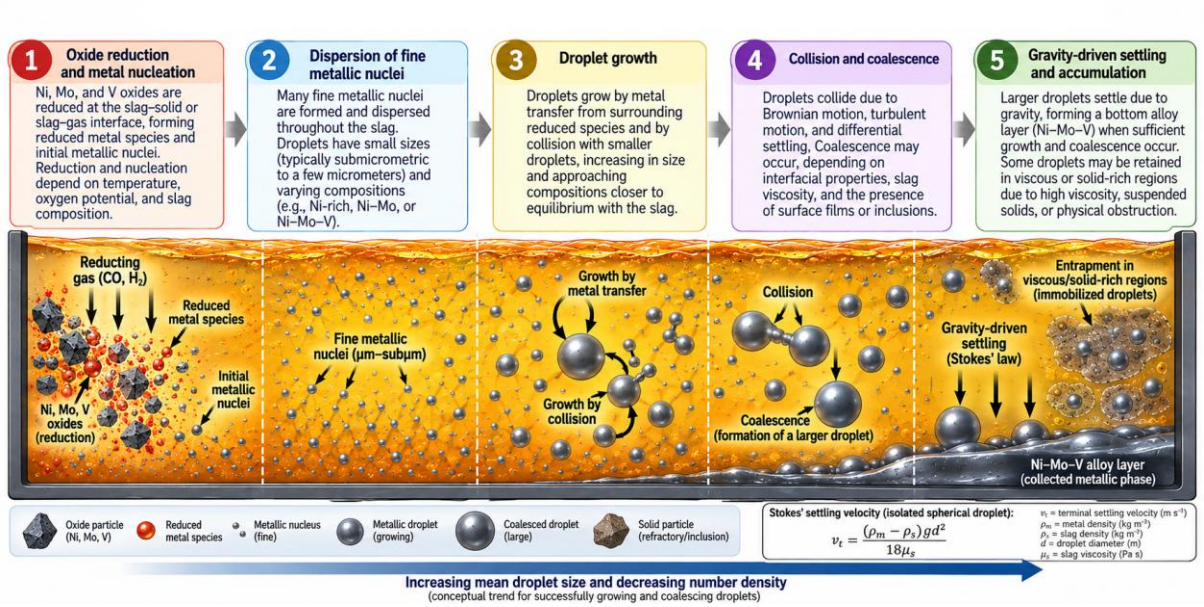

1. Introduction

Spent hydroprocessing catalysts contain economically significant Ni, Mo, and V, usually dispersed across complex oxide and carbonaceous matrices. Direct alloy recovery through reductive smelting offers a route to concentrate these metals, but reported metallization does not by itself establish recovery into a collectible metal product. Shi et al. (2023) explicitly investigated Ni–Mo–V enrichment, showing both chemical conversion and macroscopic alloy separation; their findings motivate a second question: which physical mechanisms determine whether initially formed metal reaches the alloy phase? (Shi et al., 2023; Amato et al., 2025; Liang et al., 2022).

The processes reviewed here form a causal sequence: generation of reduced metallic domains, subsequent droplet growth, modification of the interface by slag chemistry and gas, collisions and coalescence, and transport through a potentially non-Newtonian, multiphase slag. Figure 1 shows the pathway. Figure 3 isolates the strong geometric sensitivity of ideal settling to droplet diameter, whereas Figures 2 and 4 emphasize coupled controls and scale-up validation. Tables 1–3 classify evidence and identify variables that should be compared before apparent metallurgical recovery values are interpreted.

JIRRS
Journal International Review of Research Studies
Received: 19/09/2026 - **Accepted:** 26/10/2026
Vol: 01.07
DOI: 10.66104/p3c1fk38
Pages: 1-33

The contribution is not another catalog of reduction routes. Instead, it evaluates the separation mechanisms and the uncertainty introduced when transferring evidence from copper–slag, steel–slag, and matte–slag systems to Ni–Mo–V smelting. These analogies are informative for transport physics but may differ markedly in density, interfacial chemistry, redox state, viscosity, and wetting behavior (Isaksson et al., 2023b; Wang et al., 2023; Jylhä et al., 2020).

The present study differs from the broader metallurgical review by Pereira (2026b), which surveys droplet coalescence across multiple molten-metal and slag systems. Here, the unit of analysis is specifically spent hydroprocessing-catalyst-derived Ni–Mo–V reductive smelting. The review assesses alumina-rich feed and slag chemistry, Ni-rich collector-alloy formation, vanadium's more restrictive reduction behavior, the limited direct evidence from Shi et al. (2023), and the experimental measurements needed to test droplet-scale recovery during scale-up. General metal–slag physics is used to construct testable hypotheses, not to infer Ni–Mo–V-specific transport constants. This manuscript's mechanism maps, evidence tiers, and proposed verification framework are presented as a separate system-specific synthesis; the relationship of any wording or visual material to the earlier review requires a final provenance check before submission.

2. Review Methodology and Droplet Separation Evidence

The review uses a mechanism-oriented, critical narrative approach rather than claiming systematic-review status. The working bibliography contains 128 entries dated 2020–2026; the bibliographic count does not itself establish primary-source verification. Searches focused on spent catalysts, metal nucleation, alloy evolution, metal–slag interfacial tension, coalescence, settling, viscosity, CFD, and scale-up. Screening prioritized final journal publications, experimental variables, identifiable DOIs, and direct relevance to phase separation; preprints were not eligible. Because the inventory explicitly identifies incompletely verified metadata, the present manuscript should be treated as a research draft pending full primary-source reconciliation.

A three-tier evidence hierarchy is adopted: A, direct Ni–Mo–V reductive-smelting results; B, measurements or simulations of analogous molten metal–slag separation

JIRRS
Journal International Review of Research Studies
Received: 19/09/2026 - **Accepted:** 26/10/2026
Vol: 01.07
DOI: 10.66104/p3c1fk38
Pages: 1-33

mechanisms; and C, broader context on feedstock or other pyrometallurgical routes. The latter may motivate the problem but cannot substantiate a claim concerning Ni–Mo–V droplet kinetics. Table 1 summarizes this hierarchy. Shi et al. (2023) provide an example of tier A; Isaksson et al. (2023b), Wang et al. (2023), and Jylhä et al. (2020) inform tier B.

Table 1. Evidence hierarchy and permissible interpretation

Tier	Material/system	Appropriate inference	Principal limitation
A	Spent Ni–Mo–V catalysts/reduction	Specific reduction and alloy capture	Incomplete in situ droplet data
B	Copper–slag, matte–slag, steel–slag	Candidate transport mechanisms and modeling	Composition and interface differ
C	Feedstock recovery and unrelated smelting	Broader route context only	No direct droplet evidence

Note. Critical classification developed for this review; individual study categorization requires full-text verification.

Where numerical observations are compared, the underlying material, temperature, oxygen potential, slag solid fraction, analysis basis, and experimental duration must be reported together. A visually larger metal button is not equivalent to a corrected mass balance, and a recovery percentage without residual metal-in-slag speciation cannot distinguish chemically dissolved metals from retained droplets.

The A/B/C tier system is an author-developed framework for topical relevance and inferential transferability, not a formally validated evidence-quality scale or a technology-readiness scale. Tier A is restricted to direct tests of spent Ni–Mo–V catalyst reductive smelting and alloy/slag separation; work on other feedstocks, hydrometallurgy, and non-Ni–Mo–V slag systems belongs in Tier B or C as appropriate. The review is not a PRISMA-compliant systematic review. Search platforms, final search date, languages, Boolean strings, citation-chaining procedures, duplicate-removal rules, and preprint exclusions must be documented from reproducible search records rather than retrospectively reconstructed as facts.

3. Metallic Phase Nucleation during Reductive Smelting

Reduction transforms oxide-hosted species into metallic domains. Thermodynamic favorability constrains possible reactions but does not reveal where the first stable metal nuclei

JIRRS
Journal International Review of Research Studies
Received: 19/09/2026 - **Accepted:** 26/10/2026
Vol: 01.07
DOI: 10.66104/p3c1fk38
Pages: 1-33

appear or whether those nuclei are subsequently mobilized. Shi et al. (2023) demonstrated joint enrichment of Ni, Mo, and V through high-temperature carbothermal reactions and slag design; their process provides a direct, material-specific anchor but does not eliminate the need for time-resolved nucleus characterization. Analogous vanadium and iron smelting experiments show that heating history and reductant supply can alter phase assemblages and, therefore, the emergence of collector metal (Xin et al., 2020; Zhang & Chen, 2023).

Nuclei size and distribution may reflect reduction kinetics, surface heterogeneity, local supersaturation, and slag wetting. For catalyst-derived Ni–Mo–V, these remain mechanistic hypotheses until confirmed in quenched specimens. Nucleation is distinct from metallization: increased metallic iron or nickel may result from existing metal growth, new nucleation, or particle aggregation.

Quench at varied holding times under controlled gas composition, then use complementary microscopy and microanalysis to measure metal number density, size distribution, phase chemistry, and residual oxidation state. Figure 1 shows initial nuclei, coalesced droplets, and metal-layer formation as successive but nonautomatic outcomes.



JIRRS
Journal International Review of Research Studies
Received: 19/09/2026 - **Accepted:** 26/10/2026
Vol: 01.07
DOI: 10.66104/p3c1fk38
Pages: 1-33

Figure 1. Conceptual metal nucleation, growth, and gravity-driven migration within a slag layer.
Note. Original figure created for this review; schematic positions and droplet sizes are not experimental measurements.

The schematic emphasizes that droplet capture competes with immobilization in residual solids or viscous pockets. Before extrapolating, assess fine-particle detection limits, polished-section stereology, and sampling bias.

Comparative evidence and mechanistic boundaries

The literature cited for this mechanism spans catalyst-specific recovery chemistry and distinct molten-phase analogs. For the catalyst-derived material, the relevant publications cover "vanadium, molybdenum and nickel: A sustainability analysis of the extraction from ores versus recovery from spent catalysts" (Amato et al. (2025)); "pyrometallurgical reduction of copper slag with biochar for metal recovery" (Attah-Kyei et al. (2024)); "investigation of two immiscible liquids wetting at elevated temperature: Interaction between liquid FeMn alloy and liquid slag" (Bao et al. (2021)); "interfacial behavior in ferroalloys: The influence of sulfur in FeMn and SiMn systems" (Bublik et al. (2021)); "interfacial behavior in ferroalloys: The influence of FeMn slag composition" (Bublik et al. (2022)). For comparison, related studies examine "comprehensive recovery of metals in spent Ni–Mo/γ–Al_2O_3 hydrofining catalyst" (Cai et al. (2022)); "stepwise separation and recovery of molybdenum, vanadium, and nickel from spent hydrogenation catalyst" (Chen et al. (2022)); "gas–slag–matte multiphase flow and bubble dynamics in an industrial side-blown smelting furnace" (Fang et al. (2025)); "synchronous conversion and targeted separation of valuable metals from spent hydroprocessing catalysts" (Feng et al. (2024)); "high-efficiency recycling method for Mo and Ni from spent catalyst via soda roasting and solvent extraction" (Gao et al. (2022)). The remaining cited topics extend this comparison to "co-treatment of spent catalyst leaching residue with low-grade Pt/Pd and copper slag to recover valuable metals" (Gu et al. (2025)); "a leaching, solvent extraction, stripping, precipitation and calcination process for the recovery of MoO_3 and NiO from spent hydrofining catalysts" (Han et al. (2023)); "coalescence and sedimentation of liquid iron droplets during smelting reduction of converter slag with mechanical stirring" (He et al. (2020)); "fe–P alloy production from high-phosphorus oolitic iron ore via efficient pre-reduction and smelting separation" (Hu et al. (2025)); "improved

JIRRS
Journal International Review of Research Studies
Received: 19/09/2026 - **Accepted:** 26/10/2026
Vol: 01.07
DOI: 10.66104/p3c1fk38
Pages: 1-33

settling mechanisms of an industrial copper smelting slag by CaO modification" (Isaksson et al. (2023)). Further work covered in the bibliography concerns "liquid phase fraction effect on metal recovery during semi-molten low temperature reduction of pickling sludge" (Jing et al. (2025)); "cFD-DEM models for matte droplet settling in a flash smelting settler" (Jylhä et al. (2023)); "computational approaches for studying slag–matte interactions in the flash smelting furnace (FSF) settler" (Jylhä et al. (2020)); "flash smelting settler design modifications to reduce copper losses using numerical methods" (Khan et al. (2022)); "thermodynamic analysis of copper smelting, considering the impact of minor elements behavior on slag application options and Cu recovery" (Klaffenbach et al. (2021)). Additional process analogues involve "effect of pre-reduction of manganese ore by hydrogen on its smelting behavior and interaction with stable oxides" (Kumar et al. (2025)); "a review of metallurgical processes and purification techniques for recovering Mo, V, Ni, Co, Al from spent catalysts" (Liang et al. (2022)); "synergetic valorization of basic oxygen furnace slag and stone coal: Metal recovery and preparation of glass-ceramics" (Lin et al. (2021)); "a novel process for preparing ferrosilicon alloy from coal gasification coarse slag" (Liu et al. (2026)); "influence of the reduction rate of slag from oxidation process of Cu–Fe–Pb alloy during reduction (de-coppering) on its viscosity" (Madej (2025)). The remaining cited topics extend this comparison to "studies on removal of petroleum fractions from spent petrochemical catalysts to prepare them for pyrometallurgical recovery of Ni, Mo and V" (Madej et al. (2025)); "thermodynamic assessment of tin-smelting from cassiterite concentrates" (Moosavi-Khoonsari et al. (2024)); "gold recovery from smelting copper sulfide concentrate" (Moosavi-Khoonsari et al. (2024)); "separation of Li and Co from $LiCoO_2$ cathode material through aluminothermic reduction: Investigation of the thermite reaction" (Nababan et al. (2024a)); "separation of Li and Co from $LiCoO_2$ cathode material through aluminothermic reduction: Thermodynamic calculations and experimental results" (Nababan et al. (2024b)). Further work covered in the bibliography concerns "sustainable extraction of valuable metals from petroleum spent hydroprocessing catalysts using a biodegradable lixiviant" (Pathak et al. (2025)); "from vanadium–titanium magnetite to Fe–C–V alloys: A critical review of vanadium-bearing pig iron production, vanadium partitioning, refining, and metallurgical applications" (Pereira (2026)); "liquid-metal droplet coalescence in metallurgical slags: A critical review of interfacial phenomena, slag

JIRRS
Journal International Review of Research Studies
Received: 19/09/2026 - **Accepted:** 26/10/2026
Vol: 01.07
DOI: 10.66104/p3c1fk38
Pages: 1-33

properties, hydrodynamics, kinetics, and metal recovery" (Pereira (2026)); "recovery and recycling of spent Ni–Mo–V catalysts: Technologies, environmental drivers and circular economy perspectives" (Pereira (2026)); "integrated battery scrap recycling and nickel slag cleaning with methane reduction" (Ruismäki et al. (2020)). Additional process analogues involve "oxidation leaching of NiMoV alloy enriched from spent hydrogenation catalysts and solvent extraction of Mo and V" (Shi et al. (2024)); "enrichment of Ni–Mo–V via pyrometallurgical reduction from spent hydrogenation catalysts and the multi-reaction mechanism" (Shi et al. (2023)); "recovery of nickel and preparation of ferronickel alloy from spent petroleum catalyst via cooperative smelting–vitrification process with coal fly ash" (Sun et al. (2024)); "conceptual tapping model of Mn-ferroalloy furnaces" (Tangstad et al. (2022)); "recovery of valuable metals from spent HDS catalysts and comprehensive utilization of spent HDS" (Tian et al. (2026)). The remaining cited topics extend this comparison to "multiphase equilibrium relationships between copper matte and $CaO–Al_2O_3$-bearing iron silicate slags in combined smelting of WEEE and copper concentrates" (Tian et al. (2024)); "green utilization of zinc smelting slag by hydrogen reduction: Role of MgO in metal separation and recovery" (Tian et al. (2026)); "the interfacial adhesion behaviors of sedimentation zone in flash smelting based on DFT calculation (Part II)—The adhesion mechanisms of Fe_3O_4 with FeS, Ni_3S_2 and Cu_2S" (Wang et al. (2026)); "a green method to clean copper slag and rapidly recover copper resources via reduction-sulfurizing smelting and super-gravity separation at low temperature" (Wang et al. (2024)); "an eco-friendly approach for enhanced separation and efficient recovery of copper matte from molten copper smelting slag via supergravity" (Wang et al. (2025)). Further work covered in the bibliography concerns "multiphase stirring dynamics of gas–slag–matte in large-scale side-blown copper bath smelting process" (Wan et al. (2024)); "extraction and recovery of metals from spent HDS catalysts: Lab- and pilot-scale results of the overall process" (Xhaferaj et al. (2022)); "evolution of the structure and viscosity of copper slag during metallization-reduction" (Xiao et al. (2022)); "slag–metal separation and reduction behaviors of vanadium-bearing titanomagnetite metalized pellets" (Xin et al. (2020)); "investigation interfacial wetting behavior of copper matte/slag/Fe_3O_4 enriched intermediate layer during high temperature smelting" (Xu et al. (2025)). Additional process analogs involve "sustainable recovery of nickel, molybdenum, and vanadium from spent hydroprocessing catalysts by an

JIRRS
Journal International Review of Research Studies
Received: 19/09/2026 - **Accepted:** 26/10/2026
Vol: 01.07
DOI: 10.66104/p3c1fk38
Pages: 1-33

integrated selective route" (Zhang et al. (2020)); "recovery of valuable metals and production of Fe–V crude alloy from vanadium-enriched slag using aluminum dross as a reductant" (Zhang et al. (2023)); "metal recovery from spent Ni-Mo-V hydrodesulphurisation catalyst in oxalic acid media by mechanochemical treatment" (Zoraga (2024)). These contributions are complementary rather than interchangeable: recovery-route descriptions cannot determine nucleus density, whereas studies on other slags cannot establish Ni–Mo–V nucleation kinetics.

A critical measurement challenge is to distinguish new metallic nuclei from growth and merger of pre-existing domains. A minimum time-resolved quench design should sample three or more holding times under matched temperature, atmosphere, slag chemistry, and reductant conditions. Droplet number density, N_v = Ndroplets/Vslag sampled, and both number-weighted and mass- or volume-weighted diameter distributions should be reported together. Polished-section measurements require disclosure of microscopy detection thresholds, sampled slag regions, replicate variability, and the stereological method or uncertainty used to infer three-dimensional sizes from two-dimensional profiles.

4. Droplet Growth and Alloy Composition Evolution

Droplets may grow by the addition of newly reduced atoms, physical aggregation, and merger after collision. The routes have distinct signatures: direct growth increases volume without necessarily lowering droplet number; successful coalescence shifts the number distribution toward fewer, larger droplets. Chemical changes may also accompany growth if Ni, Mo, and V reduce at different rates. For Ni–Mo–V specifically, Shi et al. (2023) report alloy formation, while their subsequent alloy-leaching study demonstrates that a separated multimetallic product can be further processed (Shi et al., 2024).

Different systems illustrate why alloy composition should not be assumed constant across droplet sizes. Vanadium-bearing titanomagnetite reduction and Fe–V alloy production show that the reduction sequence and collector-phase conditions affect metal capture (Xin et al., 2020; Zhang & Chen, 2023). Their reported partition pathways should not be transplanted numerically into catalyst slags containing different alumina and flux levels.

JIRRS
Journal International Review of Research Studies
Received: 19/09/2026 - **Accepted:** 26/10/2026
Vol: 01.07
DOI: 10.66104/p3c1fk38
Pages: 1-33

A stronger dataset would pair individual droplet diameters with Ni/Mo/V composition and compare them with the bulk recovered alloy and the residual slag. In addition, the mass of each size class—not only the number of observed droplets—should be estimated because a few coarse spheres can dominate the retained metal inventory.

A Ni-rich collector hypothesis can be tested by measuring size-resolved alloy compositions xNi(d), xMo(d), xV(d), and xFe(d) at successive holding times. A shift in composition with droplet diameter is informative only when coupled with phase identification and a conserved elemental inventory; diameter–composition correlations alone do not establish a unique nucleation or coalescence history.

5. Metal–Slag Interfacial Tension and Wettability

Metal–slag interfacial tension sets part of the energy penalty for creating, deforming, and rupturing metal–slag interfaces. Wettability governs adherence to inclusions, crucible materials, refractory surfaces, and unreduced solids. Both quantities are functions of temperature, interfacial chemical potential, dissolved surface-active elements, and oxidation state. Studies on molten steel and ferralloy interfaces indicate strong sensitivity to adsorption and slag composition, but those observations do not automatically specify γ for Ni–Mo–V (Biswas et al., 2022; Bublik et al., 2022; Zhao et al., 2022).

A key conceptual distinction is that lower tension can facilitate droplet deformation or emulsification without necessarily improving net settling. Conversely, a stable interface may inhibit coalescence even when the liquid is sufficiently mobile. Oxygen and sulfur can alter interfacial reaction rates and competition for adsorption sites (Biswas et al., 2022). Figure 2 summarizes the coupled role of interface chemistry, bulk transport, and furnace flow.

JIRRS
Journal International Review of Research Studies
Received: 19/09/2026 - **Accepted:** 26/10/2026
Vol: 01.07
DOI: 10.66104/p3c1fk38
Pages: 1-33

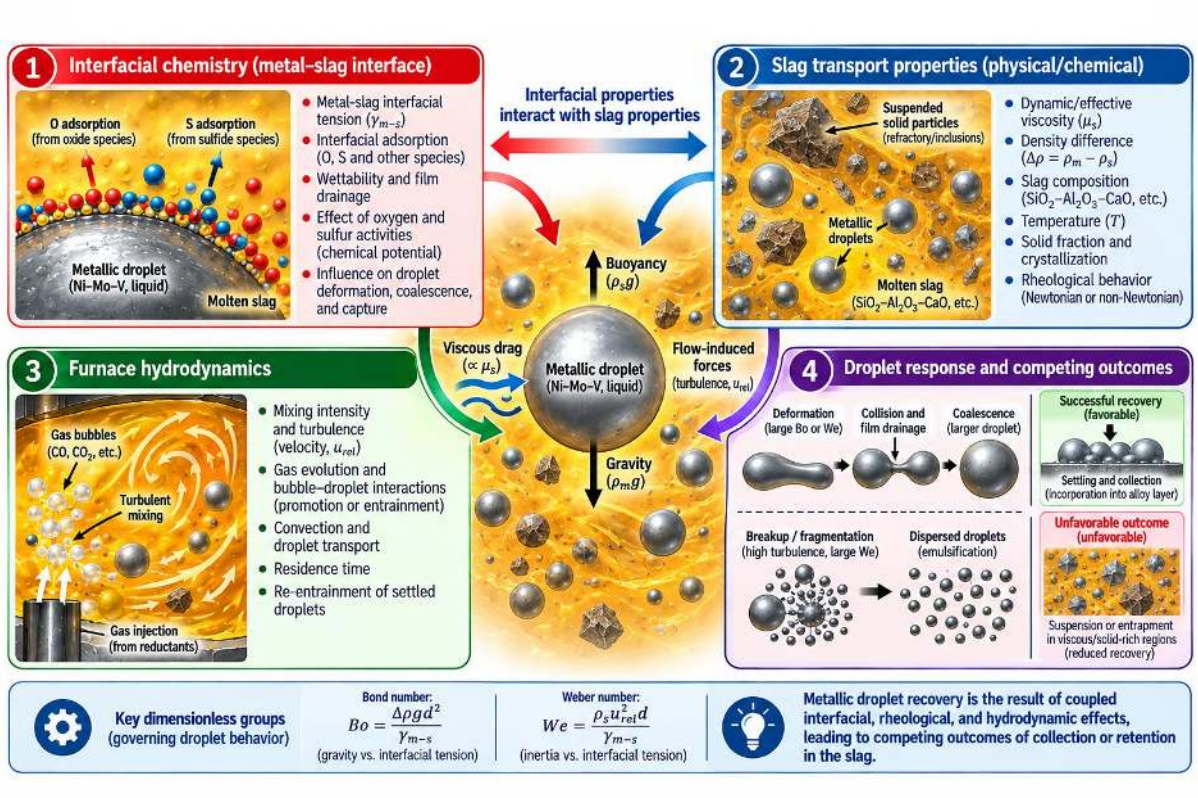

Figure 2. Coupled control of droplet capture by interfacial chemistry, slag transport, and furnace hydrodynamics.

Note. Original synthesis figure created for this review based on the cited interfacial and hydrodynamic literature.

Accordingly, contact-angle measurements on a solid substrate should not be represented as direct measurements of liquid–liquid interfacial tension. For process interpretation, the actual alloy, slag chemistry, oxygen potential, and measurement method are essential.

Interfacial analogues and limits of transfer

Interfacial studies differ in their experimental objects, from chemical adsorption to bubble-driven deformation and wetting. The cited work considers “consideration of the competitive adsorption of oxygen and sulfur on the decarburization kinetics of Fe–C droplets in oxidizing slag” (Biswas et al. (2022)); “slag electrical conductivity and its effect on mass transport and interfacial reaction kinetics” (Biswas et al. (2025)); “study on the slag-metal interfacial behavior under the impact of bubbles in different sizes” (Chang et al. (2021)); “fluid

JIRRS
Journal International Review of Research Studies
Received: 19/09/2026 - **Accepted:** 26/10/2026
Vol: 01.07
DOI: 10.66104/p3c1fk38
Pages: 1-33

dynamics studies on bottom liquid detachment from a rising bubble crossing a liquid–liquid interface" (Cheng et al. (2024)); "simulation on mass transfer at immiscible liquid interface entrained by single bubble using particle method" (Dong et al. (2020)). A separate set of investigations focuses on "in situ microscale observation of FeO_x–SiO_2 interfacial reaction" (Goto et al. (2024)); "passage of a Taylor bubble through a stratified liquid–liquid interface" (Kumar et al. (2020)); "interface-resolved simulation of bubbles–metal–slag multiphase system in a gas-stirred ladle" (Li et al. (2021)); "effects of entrained slag droplets on slag–metal interface in a gas-stirred ladle" (Liu et al. (2023)); "influence of a rising bubble on behavior of steel-slag interface" (Liu et al. (2024)). The remaining cited topics extend this comparison to "interfacial phenomena between molten iron and molten slag–Effect of nitrogen on the Marangoni convection" (Matsushita et al. (2021)); "dynamic behavior of a metal droplet in contact with slag–metal interface" (Minami et al. (2023)); "a sharp interface approach for wetting dynamics of coated droplets and soft particles" (Pelusi et al. (2023)); "effect of fluoride ions in slag on the dynamic change of the interfacial tension between liquid iron and molten slag" (Suzuki et al. (2024)); "effect of B_2O_3 addition to slag on the dynamic change behavior of interfacial tension between liquid iron and molten slag" (Suzuki et al. (2022)). Further work covered in the bibliography concerns "physical modeling of bottom-blown bubble penetration dynamics at slag/metal interface in metallurgical reactors" (Wang et al. (2025)); "kinetic model for vanadium extraction by CO_2–O_2 mixed injection based on interfacial reactions of emulsified droplets" (Wei et al. (2026)); "modelling the dissolutive wetting of slag-oxide system at high temperatures" (Yang et al. (2025)); "interfacial phenomena and reaction kinetics between high Al molten steel and CaO–SiO_2-type flux" (Zhao et al. (2022)). Their collective relevance is to define candidate interfacial mechanisms, not to assign numerical surface tensions or coalescence efficiencies to catalyst-derived alloy droplets.

6. Droplet Collision, Coalescence, and Fragmentation

Collision frequency depends on relative droplet velocities, buoyancy, and fluctuating flow fields; coalescence efficiency additionally requires drainage and rupture of the film separating the colliding droplets. The two concepts must not be conflated. Simulations of slag–matte interactions in settlers and steel–slag emulsification show that repeated encounter events

JIRRS
Journal International Review of Research Studies
Received: 19/09/2026 - **Accepted:** 26/10/2026
Vol: 01.07
DOI: 10.66104/p3c1fk38
Pages: 1-33

can coexist with prolonged entrainment, especially under active stirring (Jylhä et al., 2020; Zhang et al., 2023).

Agglomeration may be counteracted by turbulence-induced breakup or the persistence of oxide films. Bubble entrainment can lift droplets into the upper slag region, and gas-driven circulation can increase collision opportunities while preventing final settling. Hence, a higher collision rate is not a reliable proxy for higher recovery. A mechanistically interpretable experiment would vary stirring intensity at constant temperature and slag chemistry while monitoring both the time-dependent droplet distribution and metal fraction reaching the collection layer (Liu et al., 2024; Wang et al., 2023).

The most transferable finding is qualitative: surface chemistry controls whether a collision yields a stable merger; hydrodynamics controls when and where collisions occur. To apply it quantitatively to Ni–Mo–V, collision kernels, coalescence efficiencies, and size-class mass balances must be calibrated with system-specific experiments.

Droplet-dynamics analogues and uncertainty

The literature on droplet dynamics encompasses collision, film drainage, emulsification, and flow-modeling problems. Studies relevant to droplet interaction include "decarburization of bloated droplets: An experimental study to understand the kinetics of decarburization of metallic iron droplets in FeO-containing CaO–SiO_2 slags" (Biswas et al. (2021)); "investigation of iron droplets assembling in molten slag" (Lai et al. (2026)); "influence of solutal Marangoni effect on droplet behavior in metal–slag emulsion system: A numerical study" (Li et al. (2024)); "large-scale dispersed phase-resolved direct numerical simulation (LDPR-DNS) of mechanically stirred reactors: Understanding the dispersion mechanism of multiphase flow and qualifying the droplets produced" (Ma et al. (2024)); "the dynamics of bouncing, partially coalescing, liquid metal droplets in a viscous medium" (McGuan et al. (2022)). Other studies consider "influence of cryolite content on the thermal properties and coalescence efficiency of NaCl–KCl salt flux" (Milani et al. (2023)); "mathematical modeling of the ejected droplet size distribution in the vicinity of a gas–liquid impingement zone" (Mitas et al. (2022)); "modeling the residence time of metal droplets in slag during BOF steelmaking" (Mitas et al. (2023)); "experimental investigation of the

JIRRS
Journal International Review of Research Studies
Received: 19/09/2026 - **Accepted:** 26/10/2026
Vol: 01.07
DOI: 10.66104/p3c1fk38
Pages: 1-33

sedimentation behavior of metal droplets in liquid–liquid systems" (Qian et al. (2023)); "numerical simulations of the molten metal droplet formation in the electroslag remelting process with a rotating electrode" (Schubert et al. (2022)). The remaining cited topics extend this comparison to "slag–steel emulsification on a modified RH degasser" (Silva et al. (2021)); "numerical modeling of Marangoni flow between steel droplet and slag induced by concentration gradient" (Wang et al. (2025)); "hydrodynamic simulation of metal droplet settlement in molten slag" (Wang et al. (2023)); "modeling the decarburization of expansion droplets based on the solid phase ratio of slag and data fitting during BOF steelmaking process" (Xin et al. (2025)); "analysis of emulsification behavior and kinetics of reaction between high-Al molten steel and CaO–SiO_2 flux" (Zhang et al. (2023)). A valid transfer to Ni–Mo–V requires separating predicted encounter rates from observed merging events and reporting the melt chemistry and flow regime.

7. Gravitational Settling and Buoyancy Effects

Settling requires a density difference between the metal droplet and surrounding slag and enough uninterrupted residence time for the droplet to traverse the separation height. As a limiting model for an isolated rigid sphere in creeping flow, Stokes theory gives:

$$v_t = 2r^2(\rho_m - \rho_s)g / (9\mu_s) \qquad (1)$$

Here v_t is terminal speed (m s^{-1}), r is droplet radius (m), ρ_m and ρ_s are metal and slag densities (kg m^{-3}), g is gravitational acceleration (m s^{-2}), and μ_s is slag dynamic viscosity (Pa s). Equation (1) assumes a dilute suspension, a rigid sphere, low Reynolds number, Newtonian fluid behavior, and negligible wall or bubble interactions. Liquid droplets with internal circulation, deformation, or reactive interfaces can depart substantially from this model (Wang et al., 2023).

Figure 3 illustrates only mathematical sensitivity to droplet diameter and viscosity, assuming an explicitly stated example density difference; it is not a Ni–Mo–V measurement or calibrated furnace prediction. In the nominal Stokes regime, doubling droplet diameter multiplies velocity by four, while doubling viscosity halves it. However, the model may cease to apply as larger droplets deform or the Reynolds number increases.

JIRRS
Journal International Review of Research Studies

Received: 19/09/2026 - **Accepted:** 26/10/2026
Vol: 01.07
DOI: 10.66104/p3c1fk38
Pages: 1-33

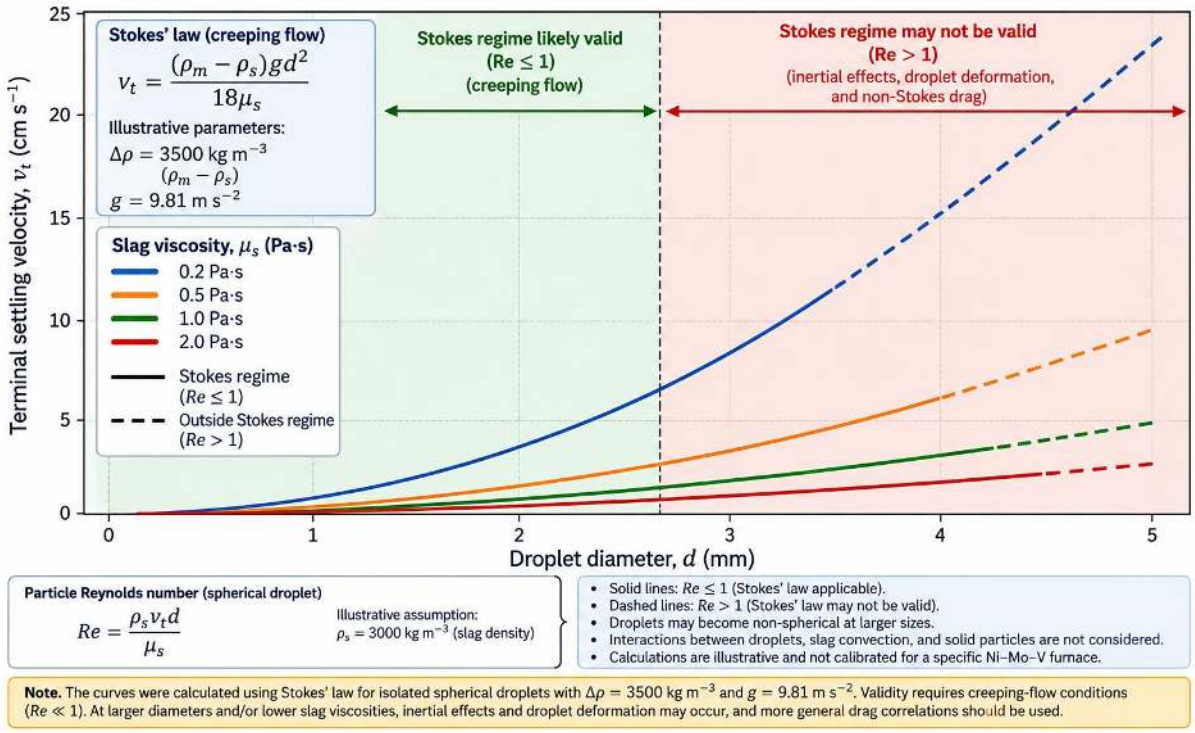

Figure 3. Illustrative ideal terminal velocity as a function of droplet diameter and slag viscosity under Stokes assumptions.

Note. Original calculated figure. Assumed density difference = 3500 kg m^{-3}, gravitational acceleration = 9.81 m s^{-2}; parameters are illustrative, not measured for Ni–Mo–V.

A more informative practical metric is the ratio of estimated vertical displacement over the residence-time distribution to the slag depth. Even this ratio must be evaluated alongside upward gas-driven currents, dead zones, and retention of droplets on solid surfaces.

Separation analogs and model applicability

The separation analogs span conventional settling, modified slag structure, and enhanced-gravity strategies. The cited investigations cover "breaking the Fe_3O_4-wrapped copper microstructure to enhance copper–slag separation" (Chi et al. (2024)); "influence of process parameters on copper content in reduced iron silicate slag in a settling furnace" (Isaksson et al. (2021)); "innovative integration of superimposed extrusion with supergravity for enhanced metallic aluminum recovery from hot dross" (Lan et al. (2026)); "settling of particle in foaming slag" (Shimasaki et al. (2024)); "sustainable recycling of pure aluminum from waste chips under supergravity-enhanced separation: A cleaning process" (Sun et al. (2024)). Additional comparisons concern "direct collection and reuse of dispersed aluminum

JIRRS
Journal International Review of Research Studies
Received: 19/09/2026 - **Accepted:** 26/10/2026
Vol: 01.07
DOI: 10.66104/p3c1fk38
Pages: 1-33

chips through salt flux and supergravity enrichment: Less salt consumption and circular economy" (Sun et al. (2025)); "sustainable recovery of metallic Al and reuse of molten salt in Al dross: Salt flux erosion and super-gravity separation" (Wang et al. (2023)); "turbulence modulation via internal baffles for intensified slag–matte separation in gas-stirred reactors" (Zhang et al. (2026)). These examples identify factors worth testing but do not establish a Ni–Mo–V settling-velocity correlation or an industrial recovery factor.

Dimensionless regime checks are required before applying rigid-sphere settling or transferring droplet dynamics from analog slags. Define $Re = \rho s\ u\ d/\mu s$, $Bo = (\rho m - \rho s)g\ d^2/\gamma$, $We = \rho s\ urel^2 d/\gamma$, and $Ca = \mu s\ urel/\gamma$, where d is droplet diameter, γ is liquid-metal/slag interfacial tension, u is the appropriate characteristic settling velocity, and urel denotes droplet–continuous-phase relative velocity. Reynolds number measures the balance of inertial and viscous stresses; Bond number compares buoyancy/gravity with capillarity; Weber number gauges inertial deformation or breakup; and Capillary number compares viscous with interfacial stresses. Their characteristic velocities and physical regimes must be specified in any application. Analog comparisons should additionally report density and viscosity ratios, solid fraction, oxygen potential, and the relevant interfacial-tension range. These quantities are proposed reporting criteria; they are not measured Ni–Mo–V values.

8. Influence of Slag Viscosity, Density, and Solid Fraction

Viscosity slows droplet motion and may suppress collision-induced coalescence by hindering film drainage. However, slag structure, solids, and droplet-size distribution mediate its relationship with metal recovery. In industrial copper slag, Isaksson et al. (2023b) linked CaO modification to changes in viscosity and droplet-size distributions, providing direct evidence that slag adjustment can improve physical separation in that system. These numerical effects cannot be adopted as performance factors for Ni–Mo–V slags without chemical equivalence.

The alumina-rich slags used for some catalyst smelting routes are compositionally distinct from fayalitic copper slags. Experimental viscosity must therefore be measured over the operating temperature and oxygen-potential ranges, with controlled solid fraction and crucible compatibility. Isaksson et al. (2023a) separately documented measurement

JIRRS
Journal International Review of Research Studies
Received: 19/09/2026 - **Accepted:** 26/10/2026
Vol: 01.07
DOI: 10.66104/p3c1fk38
Pages: 1-33

interactions between FeO_x–SiO_2–Al_2O_3 melts and crucible materials, highlighting a source of systematic uncertainty. Copper-slag metallization studies likewise show that phase evolution and apparent viscosity may evolve together (Xiao et al., 2022).

Table 2 provides a practical measurement matrix. Viscosity is not a single transferable constant: cooling, crystallization, gas bubbles, and solids can create yield-stress or shear-dependent behavior, undermining direct use of Equation (1).

Table 2. Variables required for comparable metal–slag separation experiments

Measurement	Unit / descriptor	Why it matters
Droplet diameter distribution	µm; number- and mass-weighted	Growth, coalescence, and entrained metal
Slag dynamic viscosity	Pa s; temperature and shear specified	Settling resistance and film drainage
Metal/slag density	kg m^{-3} at process T	Buoyant driving force
Interfacial tension	N m^{-1}; oxygen potential specified	Deformation, wetting, breakup
Solid fraction and mineralogy	Vol. fraction; phase identities	Hindrance and non-Newtonian rheology
Residence-time distribution	s or min; distribution	Time available to capture droplets

Note. Original critical synthesis table. Measurements must refer to the same thermal, chemical, and sampling state to be mutually comparable.

The table distinguishes essential measured variables from convenient surrogates. Reporting nominal basicity alone does not adequately define viscosity, and bulk analysis of the slag cannot establish whether metal losses are physically entrained or dissolved.

Slag-property evidence and experimental comparability

Studies pertinent to rheology describe both bulk-liquid properties and the changes caused by solids, temperature, and slag chemistry. The relevant topics include “additive effect of Al_2O_3, CaO, and MgO on the viscosity of FeO_x–SiO_2 slag melt (x = 1.0–1.5)” (Eguchi et al. (2023)); “effect of FeO/SiO2 ratio, Al2O3, and CaO content on viscosity and ionic structure in FeO–SiO2–Al2O3–CaO–MgO–Cr2O3 melts” (Isaksson et al. (2025)); “interactions of crucible materials with an FeO_x–SiO_2–Al_2O_3 melt and their influence on viscosity measurements” (Isaksson et al. (2023)); “slag composition control indices in high-temperature metallurgy: A critical review of viscosity, conductivity, corrosion, and refractory wear” (Pereira (2026)); “rheological behavior of slag–melilite suspensions in pyrometallurgical

JIRRS
Journal International Review of Research Studies
Received: 19/09/2026 - **Accepted:** 26/10/2026
Vol: 01.07
DOI: 10.66104/p3c1fk38
Pages: 1-33

secondary lead smelter systems" (Vergote et al. (2025)). Other investigations address "mechanistic insights into metallic iron-induced changes in viscosity, structure, and iron agglomeration of fixed-bed gasifier slag" (Wu et al. (2026)). Their applicability depends on whether they reproduce the same phases, measurement temperature, oxygen potential, and shear conditions.

For an element M ∈ {Ni, Mo, V, Fe}, define reduction efficiency R_M,red = 100 m_M,reduced/m_M,feed and recovered-alloy efficiency R_M,alloy = 100 m_M,collected alloy/m_M,feed, provided that both quantities are calculated on the same elemental input basis. The residual slag inventory should be speciated as m_M,slag = m_M,dissolved + m_M,entrained droplets + m_M,unreduced/solid, with operationally defined analytical separation methods. Closure requires C_M = 100(m_M,alloy + m_M,slag + m_M,dust/other)/m_M,feed, accompanied by an uncertainty estimate. Differences between reduction and collection efficiencies can suggest physical capture losses but cannot be assigned solely to droplet entrainment unless other inventory terms and measurement biases have been reconciled. Experimental reporting should also document melt liquid fraction, mineral phase identities, temperature-dependent viscosity, oxygen potential, reductant/carbon condition, melt densities, and composition- and time-dependent interfacial tension where measurable.

9. Hydrodynamic Modeling and Residence-Time Effects

Computational fluid dynamics (CFD), population-balance models, and particle-tracking approaches can integrate settling, collision, and turbulent circulation, but each is only as strong as its constitutive inputs. Jylhä et al. (2020) modeled slag–matte processes in flash-smelting settlers, whereas Wang et al. (2023) explored molten-metal droplet settlement with interfacial effects and different turbulence descriptions. Both are relevant mechanism analogues, not independently validated models of catalyst-derived Ni–Mo–V slag.

A reactor-scale prediction must impose realistic spatial fields of temperature, composition, viscosity, bubbles, and velocity, as well as an inlet size distribution and plausible collision efficiencies. Using one fixed, mean droplet size biases predicted separation because settling speed is nonlinear in size. A narrow mean residence time similarly conceals early short-circuiting and zones with prolonged local retention.

JIRRS
Journal International Review of Research Studies
Received: 19/09/2026 - **Accepted:** 26/10/2026
Vol: 01.07
DOI: 10.66104/p3c1fk38
Pages: 1-33

Figure 4 proposes a validation loop in which microscopy, slag characterization, residence-time testing, and reconciled mass balance inform and test the model. Calibration and validation should use different data sets; agreement obtained by adjusting an unmeasured coalescence rate alone is not predictive evidence.

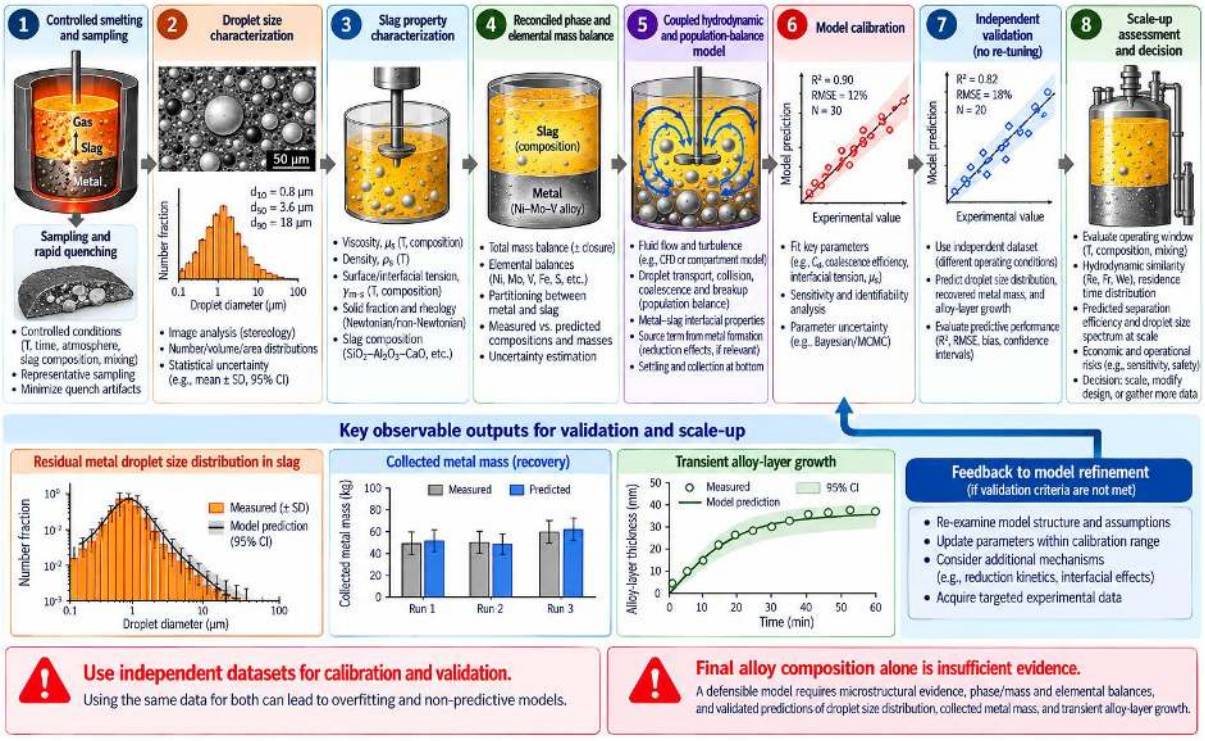

Figure 4. Minimum evidence chain for defensible model validation and metal–slag separation scale-up.

Note. Original framework prepared for this review; no published figure reproduced or adapted.

Before transferring a model, at least three observables should be checked: residual metal size spectrum in the slag, collected metal mass, and transient layer growth. None can be inferred reliably from a final alloy assay alone.

Hydrodynamic evidence for scale-up

Hydrodynamic analogues are useful for specifying reactor-scale questions rather than predicting an alloy yield without calibration. The cited publications investigate “development and design of the first industrial magnetohydrodynamic slag-cleaning reactor from execution and analysis of pilot plant tests through coupled CFD simulations” (Kalisch et al. (2023)); “physical and mathematical modeling of flow structures of liquid steel in ladle stirring

JIRRS
Journal International Review of Research Studies
Received: 19/09/2026 - **Accepted:** 26/10/2026
Vol: 01.07
DOI: 10.66104/p3c1fk38
Pages: 1-33

operations" (Morales et al. (2020)); "numerical study of binary trickle flow of liquid iron and molten slag in coke bed by smoothed particle hydrodynamics" (Natsui et al. (2020)). Transfer requires residence-time distributions and phase-resolved mass balances under comparable gas evolution and mixing conditions.

The coalescence contribution to a population balance should distinguish collision encounter rate from success probability, Kcoal = Kcoll Pcoal, and explicitly consider droplet generation, growth, breakup, and settling/removal. A dimensionless screening ratio Πs = veff tavail/Hslag may compare effective displacement to slag depth, but veff must first be supported by hydrodynamic validation; Πs > 1 alone cannot establish recovery in the presence of recirculation, short-circuiting, gas holdup, dead zones, or re-entrainment. Model calibration and validation must use independent data, with tests against droplet-size distributions, residual metal speciation/inventory, collected alloy-layer mass, transient layer growth, and residence-time distributions E(t). Prediction uncertainty, sensitivity, grid/time-step behavior, and assumptions for turbulence, drag, coalescence, breakup, and reaction coupling should be made explicit when such models are applied.

10. Critical Separation Mechanisms and Scale-Up Limitations

A mechanism-based scale-up framework must preserve the competition among reduction, droplet coalescence, settling, and furnace-driven remixing. The strongest directly applicable Ni–Mo–V evidence concerns enrichment under reductive smelting and metal-layer separation (Shi et al., 2023). The richest droplet-scale evidence derives mainly from other systems. This evidence asymmetry is the central limitation of the current literature; it does not justify an assumed universal transfer coefficient across slags.

Table 3 identifies unresolved questions and discriminating experiments. A reliable comparison should distinguish direct chemical unrecovery, chemically dissolved metal retained in slag, and physically entrained droplets. Each category requires different interventions: reductant chemistry, slag thermodynamics, or hydrodynamics/coalescence control. Without this separation, an observed improvement after flux addition is not mechanistically attributable to viscosity alone (Isaksson et al., 2023b; Wang et al., 2023).

JIRRS
Journal International Review of Research Studies
Received: 19/09/2026 - **Accepted:** 26/10/2026
Vol: 01.07
DOI: 10.66104/p3c1fk38
Pages: 1-33

Table 3. Scale-up questions and tests prioritized for Ni–Mo–V catalyst smelting

Uncertainty	Test needed	Decision enabled
New nuclei vs growth	Time-resolved quench + SEM-EDS	Locate reduction bottleneck
Retained droplets vs dissolved metal	Polished-section mapping + chemical extraction	Select cleanup mechanism
Viscosity/solids interaction	High-temperature rheometry + phase analysis	Set thermal and flux window
Coalescence vs breakup	Controlled stirring + temporal droplet counts	Choose agitation regime
Model representativeness	Residence-time distribution + independent mass balance	Support scale-up claims

Note. Original evidence-gap framework; suggested tests are methodological recommendations, not results from the reviewed studies.

For equipment selection, the best available criterion is not maximum mixing intensity but adequate reaction rate followed by a physically protected disengagement period. Compartmentation, settling zones, tapping configuration, and stable thermal fields deserve explicit comparison. A technologically mature operation in a copper smelter does not establish a technology readiness level for untested Ni–Mo–V separation hardware; no numeric TRL is assigned here.

Future work should publish open size-resolved metallurgical balances, replicate slag rheology data, the oxygen potential of the metal–slag interface, and experimentally characterized flow fields. The intended result is a separation model whose error bounds are measured rather than inferred from a plausible visual resemblance between furnace systems.

Related process evidence and scope limitations

Beyond droplet transport, several publications describe process integration, material valorization, and operating constraints. These contributions address “solubility of gold in FeO_x–SiO_2–Al_2O_3 slags at 1300 °C” (Avarmaa et al. (2025)); “adoption of hydrogen as a climate-neutral reducing agent for recovering metals from copper slag” (Chen et al. (2025)); “effect of pyro-processing conditions on impurity removal and precious metal enrichment in waste printed circuit board (WPCB) recycling process” (Heo et al. (2022)); “sustainable and comprehensive utilization of copper slag: A review and critical analysis” (Klaffenbach et al. (2023)); “review on operation of spinel-containing slags of the non-ferrous metallurgy” (Kleeberg (2022)). Other relevant topics include “recovery of heavy metals from copper slag

JIRRS
Journal International Review of Research Studies
Received: 19/09/2026 - **Accepted:** 26/10/2026
Vol: 01.07
DOI: 10.66104/p3c1fk38
Pages: 1-33

by slow cooling: Mechanism of matte growth and transformation behaviors of heavy metals" (Kuang et al. (2025)); "study of inclusions-removal and slag–metal dispersion phenomenon in gas-stirred ladle" (Liu et al. (2024)); "green and efficient recovery of valuable metals from waste copper slag via co-modification with CaO and Na_2O" (Liu et al. (2023)); "basic oxygen steelmaking slag: Formation, reaction, and energy and material recovery" (Li et al. (2022)); "implications of direct use of slag from ironmaking processes as molten oxide electrolyte" (Martín Treceño et al. (2021)). The remaining cited topics extend this comparison to "melting behavior of hydrogen-reduced vanadium-bearing titanomagnetite ironsand pellets in a laboratory-scale electrode smelter" (Mendoza et al. (2026)); "solid salt fluxes for molten aluminum processing—A review" (Milani et al. (2023)); "linear stability of a thin fluid film interacting with its surrounding bulk fluid" (Mirjalili et al. (2021)); "chromium in slag from SOEL interconnects remelting: Characterization and recycling potential" (Mongoljiibuu et al. (2025)); "experimental investigation of hydrogen-based DRI melting behavior coupled with thermodynamic prediction for optimization of carburizing agents and flux blending conditions" (Park et al. (2026)). Further work covered in the bibliography concerns "scale-up in mineral processing: From mechanism preservation to flowsheet-scale transferability—A critical review and the MINESCALE framework" (Pereira (2026)); "investigation of liquid–liquid reaction phenomena of aluminum in calcium silicate slag" (Philipson et al. (2024)); "processing of a zinc leach residue by a non-fossil reductant" (Rämä et al. (2023)); "pyrometallurgical valorization of Waelz, fayalite, and Linz–Donawitz slag mixtures" (Romero et al. (2026)); "optimal hot metal desulphurisation slag considering iron loss and sulphur removal capacity part I: Fundamentals" (Schrama et al. (2021)). Additional process analogues involve "hidden phenomena during transient reaction trajectories in liquid metals processing" (Spooner et al. (2020)); "development of an integrated process flowsheet to recover valuable metals from waste cathode ray tubes and printed circuit boards" (Tsebe et al. (2024)); "joint utilization and harmless elimination of aluminum dross and refined magnesium slag to simultaneously recover metallic aluminum and fusing agent" (Wang et al. (2024)); "study of the relationship between solid phase transformation and flow behavior transitions driven by carbothermal reaction in slag of BGL gasification" (Wu et al. (2025)). They provide process context and candidate tests; they do not independently verify Ni–Mo–V droplet mechanisms.

JIRRS
Journal International Review of Research Studies
Received: 19/09/2026 - **Accepted:** 26/10/2026
Vol: 01.07
DOI: 10.66104/p3c1fk38
Pages: 1-33

The proposed equipment strategy of adequate reaction intensity followed by a protected disengagement interval is a design hypothesis rather than a demonstrated optimum for catalyst-derived Ni–Mo–V melts. Validation should assess stirring geometry and power, gas-generation rate and bubble transport, slag depth, solid adhesion and refractory wetting, tapping-induced re-entrainment, and effects of flux additions on both rheology and chemical equilibria. Kilogram-scale outcomes should not be represented as pilot or full-scale validation, and no numeric integrated-process TRL is inferred from the maturity of analogous furnaces or computational methods.

11. Conclusions

Recovery of Ni–Mo–V by reductive smelting is ultimately controlled by both chemical formation of alloy and its physical transport to a collectable phase. Nucleation, size-dependent growth, collision efficiency, interfacial chemistry, slag viscosity, and residence-time distributions are coupled and cannot be independently optimized by equilibrium calculations alone. Stokes theory is useful for bounding diameter and viscosity sensitivity but cannot replace multiphase characterization of deformable metal droplets in reactive slags. The present evidence supports a mechanism-based conceptual framework while revealing a shortage of directly validated droplet-scale Ni–Mo–V data. Future experimental programs should therefore combine time-resolved imaging, phase-specific balances, high-temperature property measurements, and independent reactor-scale validation before asserting transferable industrial separation efficiencies. Equally important, dissolved metal in slag, unreduced metal-bearing particles, and reduced alloy droplets remaining entrained represent distinct loss mechanisms and demand separate process interventions. Quantitative scale-up therefore requires independently verified elemental closure and time-resolved characterization of the droplet population, alongside slag and flow-field properties.

Declarations

Funding

Funding status requires author confirmation before submission.

JIRRS
Journal International Review of Research Studies

Received: 19/09/2026 - **Accepted:** 26/10/2026
Vol: 01.07
DOI: 10.66104/p3c1fk38
Pages: 1-33

Conflict of Interest

Conflict-of-interest status requires author confirmation before submission.

Data Availability

No new experimental datasets were generated. The material reviewed is drawn from published sources listed in the References; source identifiers and bibliographic accuracy require final primary-source audit before journal submission.

Author Contributions

Author contribution details must be confirmed against the actual research, screening, writing, graphics, and revision workflow before submission.

References

Amato, A., Ippolito, N. M., D'Arcangelo, M., Becci, A., Innocenzi, V., & Ferella, F. (2025). Vanadium, molybdenum and nickel: A sustainability analysis of the extraction from ores versus recovery from spent catalysts. Journal of Cleaner Production, 515, 145817. https://doi.org/10.1016/j.jclepro.2025.145817

Attah-Kyei, D., Sukhomlinov, D., Klemettinen, L., Michallik, R., O'Brien, H., Taskinen, P., & Lindberg, D. (2024). Pyrometallurgical reduction of copper slag with biochar for metal recovery. Journal of Sustainable Metallurgy, 10, 1170–1187. https://doi.org/10.1007/s40831-024-00885-4

Avarmaa, K., Klemettinen, L., Michallik, R. M., & Lindberg, D. (2025). Solubility of gold in FeO_x–SiO_2–Al_2O_3 slags at 1300 °C. Mineral Processing and Extractive Metallurgy Review, 46(8), 858–864. https://doi.org/10.1080/08827508.2025.2454688

Bao, S., Tangstad, M., Tang, K., Einarsrud, K. E., Syvertsen, M., Onsøien, M. I., Kudyba, A., & Bublik, S. (2021). Investigation of two immiscible liquids wetting at elevated temperature: Interaction between liquid FeMn alloy and liquid slag. Metallurgical and Materials Transactions B, 52, 2847–2858. https://doi.org/10.1007/s11663-021-02222-6

Biswas, J., Gu, K., & Coley, K. S. (2021). Decarburization of bloated droplets: An experimental study to understand the kinetics of decarburization of metallic iron droplets in FeO-containing CaO–SiO_2 slags. Metallurgical and Materials Transactions B, 52(6), 4215–4229. https://doi.org/10.1007/s11663-021-02344-x

Biswas, J., Gu, K., & Coley, K. S. (2022). Consideration of the competitive adsorption of oxygen and sulfur on the decarburization kinetics of Fe–C droplets in oxidizing slag. Metallurgical and Materials Transactions B, 53(6), 4087–4104. https://doi.org/10.1007/s11663-022-02669-1

JIRRS
Journal International Review of Research Studies

Received: 19/09/2026 - **Accepted:** 26/10/2026
Vol: 01.07
DOI: 10.66104/p3c1fk38
Pages: 1-33

Biswas, J., Hazaveh, P. K., & Coley, K. S. (2025). Slag electrical conductivity and its effect on mass transport and interfacial reaction kinetics. Steel Research International, 96(4), Article 2300701. https://doi.org/10.1002/srin.202300701

Bublik, S., Bao, S., Tangstad, M., & Einarsrud, K. E. (2021). Interfacial behaviour in ferroalloys: The influence of sulfur in FeMn and SiMn systems. Metallurgical and Materials Transactions B, 52, 3624–3645. https://doi.org/10.1007/s11663-021-02323-2

Bublik, S., Tangstad, M., & Einarsrud, K. E. (2022). Interfacial behaviour in ferroalloys: The influence of FeMn slag composition. Metallurgical and Materials Transactions B, 53(5), 3276–3291. https://doi.org/10.1007/s11663-022-02605-3

Cai, Y., Ma, L., Xi, X., Nie, Z., & Yang, Z. (2022). Comprehensive recovery of metals in spent Ni–Mo/γ–Al_2O_3 hydrofining catalyst. Hydrometallurgy, 208, 105800. https://doi.org/10.1016/j.hydromet.2021.105800

Chang, S., Zou, Z., Liu, J., Isac, M., Cao, X. E., Su, X., & Guthrie, R. I. L. (2021). Study on the slag-metal interfacial behavior under the impact of bubbles in different sizes. Powder Technology, 387, 125–135. https://doi.org/10.1016/j.powtec.2021.04.018

Cheng, X., Qing, G., Zhao, Z., & Zhao, B. (2024). Fluid dynamics studies on bottom liquid detachment from a rising bubble crossing a liquid–liquid interface. Metals, 14(9), 1005. https://doi.org/10.3390/met14091005

Chen, M., Sukhomlinov, D., Taskinen, P., Hamuyuni, J., Tiljander, M., Lindgren, M., & Lindberg, D. (2025). Adoption of hydrogen as a climate-neutral reducing agent for recovering metals from copper slag. Metallurgical and Materials Transactions B, 56, 1897–1913. https://doi.org/10.1007/s11663-025-03444-8

Chen, R., Feng, C., Tan, J., Zhang, C., Yuan, S., Liu, M., Hu, H., Li, Q., & Hu, J. (2022). Stepwise separation and recovery of molybdenum, vanadium, and nickel from spent hydrogenation catalyst. Hydrometallurgy, 213, 105910. https://doi.org/10.1016/j.hydromet.2022.105910

Chi, X., Liu, H., Xia, J., Chen, H., Yu, X., Weng, W., & Zhong, S. (2024). Breaking the Fe_3O_4-wrapped copper microstructure to enhance copper–slag separation. International Journal of Minerals, Metallurgy and Materials, 31(10), 2312–2325. https://doi.org/10.1007/s12613-024-2861-4

Dong, C., Guo, K., Cai, Q., Chen, R., Tian, W., Qiu, S., & Su, G. H. (2020). Simulation on mass transfer at immiscible liquid interface entrained by single bubble using particle method. Nuclear Engineering and Technology, 52(6), 1172–1179. https://doi.org/10.1016/j.net.2019.11.023

Eguchi, T., Nishioka, N., & Takebe, H. (2023). Additive effect of Al_2O_3, CaO, and MgO on the viscosity of FeO_x–SiO_2 slag melt (x = 1.0–1.5). Journal of Sustainable Metallurgy, 9(4), 1487–1498. https://doi.org/10.1007/s40831-023-00741-x

JIRRS
Journal International Review of Research Studies

Received: 19/09/2026 - **Accepted:** 26/10/2026
Vol: 01.07
DOI: 10.66104/p3c1fk38
Pages: 1-33

Fang, W., Wan, Z., Hu, Z., Wang, Y., Shi, P., Huang, J., Zhong, L., & Li, M. (2025). Gas–slag–matte multiphase flow and bubble dynamics in an industrial side-blown smelting furnace. Physics of Fluids, 37(8), 083356. https://doi.org/10.1063/5.0284052

Feng, C., Zhu, P., Zhang, L., Yu, J., Zheng, C., Luo, J., Tan, J., & Hu, J. (2024). Synchronous conversion and targeted separation of valuable metals from spent hydroprocessing catalysts. Journal of Cleaner Production, 144064. https://doi.org/10.1016/j.jclepro.2024.144064

Gao, B., Jiang, H., Zeng, M., Peng, M., Hu, L., Zhang, W., & Mao, L. (2022). High-efficiency recycling method for Mo and Ni from spent catalyst via soda roasting and solvent extraction. Journal of Cleaner Production, 367, 132976. https://doi.org/10.1016/j.jclepro.2022.132976

Goto, Y., Kawanishi, S., Natsui, S., Takahashi, J.-I., & Nogami, H. (2024). In situ microscale observation of FeO_x–SiO_2 interfacial reaction. Metallurgical and Materials Transactions B, 55(3), 1735–1753. https://doi.org/10.1007/s11663-024-03063-9

Gu, H., Tan, C., Yu, Y., Jiang, W., Wang, H., Hu, J., & Wang, H. (2025). Co-treatment of spent catalyst leaching residue with low-grade Pt/Pd and copper slag to recover valuable metals. Separation and Purification Technology, 375, Article 133792. https://doi.org/10.1016/j.seppur.2025.133792

Han, Y., Chen, J., Deng, Y., Liu, T., & Li, H. (2023). A leaching, solvent extraction, stripping, precipitation and calcination process for the recovery of MoO_3 and NiO from spent hydrofining catalysts. Hydrometallurgy, Article 106046. https://doi.org/10.1016/j.hydromet.2023.106046

He, M., Wang, N., Hou, Q., Chen, M., & Yu, H. (2020). Coalescence and sedimentation of liquid iron droplets during smelting reduction of converter slag with mechanical stirring. Powder Technology, 362, 550–558. https://doi.org/10.1016/j.powtec.2019.12.020

Heo, J., Park, J., & Park, J. H. (2022). Effect of pyro-processing conditions on impurity removal and precious metal enrichment in waste printed circuit board (WPCB) recycling process. Resources, Conservation and Recycling, 179, Article 106068. https://doi.org/10.1016/j.resconrec.2021.106068

Hu, M., Zhu, D., Pan, J., Guo, Z., Yang, C., Li, S., & Cao, W. (2025). Fe–P alloy production from high-phosphorus oolitic iron ore via efficient pre-reduction and smelting separation. Minerals, 15(8), Article 778. https://doi.org/10.3390/min15080778

Isaksson, J., Andersson, A., Lennartsson, A., Gyakwaa, F., Shu, Q., & Samuelsson, C. (2025). Effect of FeO/SiO2 ratio, Al2O3, and CaO content on viscosity and ionic structure in FeO–SiO2–Al2O3–CaO–MgO–Cr2O3 melts. Metallurgical and Materials Transactions B, 56, 2573–2586. https://doi.org/10.1007/s11663-025-03510-1

JIRRS
Journal International Review of Research Studies

Received: 19/09/2026 - **Accepted:** 26/10/2026
Vol: 01.07
DOI: 10.66104/p3c1fk38
Pages: 1-33

Isaksson, J., Andersson, A., Lennartsson, A., & Samuelsson, C. (2023). Interactions of crucible materials with an FeO_x–SiO_2–Al_2O_3 melt and their influence on viscosity measurements. Metallurgical and Materials Transactions B, 54, 3526–3541. https://doi.org/10.1007/s11663-023-02930-1

Isaksson, J., Andersson, A., Vikström, T., Lennartsson, A., & Samuelsson, C. (2023). Improved settling mechanisms of an industrial copper smelting slag by CaO modification. Journal of Sustainable Metallurgy, 9, 1378–1389. https://doi.org/10.1007/s40831-023-00733-x

Isaksson, J., Vikström, T., Lennartsson, A., & Samuelsson, C. (2021). Influence of process parameters on copper content in reduced iron silicate slag in a settling furnace. Metals, 11(6), 992. https://doi.org/10.3390/met11060992

Jing, B., Tan, J., Li, Q., & Liang, C. (2025). Liquid phase fraction effect on metal recovery during semi-molten low temperature reduction of pickling sludge. Journal of Sustainable Metallurgy, 11(4), 4575–4584. https://doi.org/10.1007/s40831-025-01282-1

Jylhä, J.-P., & Jokilaakso, A. (2023). CFD-DEM models for matte droplet settling in a flash smelting settler. Heliyon, 9(11), e21570. https://doi.org/10.1016/j.heliyon.2023.e21570

Jylhä, J.-P., Khan, N. A., & Jokilaakso, A. (2020). Computational approaches for studying slag–matte interactions in the flash smelting furnace (FSF) settler. Processes, 8(4), 485. https://doi.org/10.3390/pr8040485

Kalisch, M., Friedrich, B., & Reuter, M. A. (2023). Development and design of the first industrial magnetohydrodynamic slag-cleaning reactor from execution and analysis of pilot plant tests through coupled CFD simulations. Metallurgical and Materials Transactions B, 54, 1017–1042. https://doi.org/10.1007/s11663-023-02758-9

Khan, N. A., & Jokilaakso, A. (2022). Flash smelting settler design modifications to reduce copper losses using numerical methods. Processes, 10(4), 784. https://doi.org/10.3390/pr10040784

Klaffenbach, E., Montenegro, V., Guo, M., & Blanpain, B. (2023). Sustainable and comprehensive utilization of copper slag: A review and critical analysis. Journal of Sustainable Metallurgy, 9(2), 468–496. https://doi.org/10.1007/s40831-023-00683-4

Klaffenbach, E., Mostaghel, S., Guo, M., & Blanpain, B. (2021). Thermodynamic analysis of copper smelting, considering the impact of minor elements behavior on slag application options and Cu recovery. Journal of Sustainable Metallurgy, 7(2), 664–683. https://doi.org/10.1007/s40831-021-00354-2

Kleeberg, C. (2022). Review on operation of spinel-containing slags of the non-ferrous metallurgy. Materials Science and Technology, 38(10), 607–621. https://doi.org/10.1080/02670836.2022.2062812

JIRRS
Journal International Review of Research Studies

Received: 19/09/2026 - **Accepted:** 26/10/2026
Vol: 01.07
DOI: 10.66104/p3c1fk38
Pages: 1-33

Kuang, B., Yu, Y., Hu, J., Dou, Z., Wang, H., Yang, S., & Liu, H. (2025). Recovery of heavy metals from copper slag by slow cooling: Mechanism of matte growth and transformation behaviors of heavy metals. Separation and Purification Technology, 361, 131327. https://doi.org/10.1016/j.seppur.2024.131327

Kumar, P., & Safarian, J. (2025). Effect of pre-reduction of manganese ore by hydrogen on its smelting behavior and interaction with stable oxides. Journal of Sustainable Metallurgy, 11(3), 2980–3000. https://doi.org/10.1007/s40831-025-01162-8

Kumar, R., Rohilla, L., & Das, A. K. (2020). Passage of a Taylor bubble through a stratified liquid–liquid interface. Industrial & Engineering Chemistry Research, 59(9), 3757–3771. https://doi.org/10.1021/acs.iecr.9b04235

Lai, C., Jing, B., Tan, J., & Li, Q. (2026). Investigation of iron droplets assembling in molten slag. Colloids and Surfaces A: Physicochemical and Engineering Aspects. https://doi.org/10.1016/j.colsurfa.2026.139463

Lan, X., Gao, J., Feng, G., Li, X., & Guo, Z. (2026). Innovative integration of superimposed extrusion with supergravity for enhanced metallic aluminum recovery from hot dross. Journal of Materials Research and Technology, 41, 2070–2080. https://doi.org/10.1016/j.jmrt.2026.01.141

Liang, X., Tang, J., Li, L., Wu, Y., & Sun, Y. (2022). A review of metallurgical processes and purification techniques for recovering Mo, V, Ni, Co, Al from spent catalysts. Journal of Cleaner Production, 376, 134108. https://doi.org/10.1016/j.jclepro.2022.134108

Li, M., Li, L., Shao, L., Li, W., & Zou, Z. (2024). Influence of solutal Marangoni effect on droplet behavior in metal–slag emulsion system: A numerical study. JOM, 76(11), 6433–6445. https://doi.org/10.1007/s11837-024-06575-6

Lin, Y., Yan, B., Shu, Q., & Fabritius, T. (2021). Synergetic valorization of basic oxygen furnace slag and stone coal: Metal recovery and preparation of glass-ceramics. Waste Management, 135, 158–166. https://doi.org/10.1016/j.wasman.2021.08.044

Li, Q., & Pistorius, P. C. (2021). Interface-resolved simulation of bubbles–metal–slag multiphase system in a gas-stirred ladle. Metallurgical and Materials Transactions B, 52(3), 1532–1549. https://doi.org/10.1007/s11663-021-02121-w

Liu, C., Yao, S., Yang, X., Tang, C., & Xing, P. (2026). A novel process for preparing ferrosilicon alloy from coal gasification coarse slag. Silicon, 18(3–4), 1193–1206. https://doi.org/10.1007/s12633-025-03593-0

Liu, Y., Cheng, S., & Liu, T. (2023). Effects of entrained slag droplets on slag–metal interface in a gas-stirred ladle. ISIJ International, 63(6), 1017–1024. https://doi.org/10.2355/isijinternational.ISIJINT-2022-164

Liu, Y., Cheng, S., & Liu, T. (2024). Study of inclusions-removal and slag–metal dispersion phenomenon in gas-stirred ladle. International Journal of Chemical Reactor Engineering, 22(7), 843–853. https://doi.org/10.1515/ijcre-2024-0090

JIRRS
Journal International Review of Research Studies

Received: 19/09/2026 - **Accepted:** 26/10/2026
Vol: 01.07
DOI: 10.66104/p3c1fk38
Pages: 1-33

Liu, Y., Cheng, S., & Liu, T. (2024). Influence of a rising bubble on behavior of steel-slag interface. Iron and Steel, 59(2), 75–84. https://doi.org/10.13228/j.boyuan.issn0449-749x.20230306

Liu, Y., Xu, L., & Chen, M. (2023). Green and efficient recovery of valuable metals from waste copper slag via co-modification with CaO and Na_2O. Process Safety and Environmental Protection, 180, 959–971. https://doi.org/10.1016/j.psep.2023.10.061

Li, Z., Li, J., Spooner, S., & Seetharaman, S. (2022). Basic oxygen steelmaking slag: Formation, reaction, and energy and material recovery. Steel Research International, 93(3), Article 2100167. https://doi.org/10.1002/srin.202100167

Madej, P. (2025). Influence of the reduction rate of slag from oxidation process of Cu–Fe–Pb alloy during reduction (de-coppering) on its viscosity. Metallurgical and Materials Transactions B, 56, 833–851. https://doi.org/10.1007/s11663-024-03381-y

Madej, P., Czech, A., Pęcak, K., & Cybulski, A. (2025). Studies on removal of petroleum fractions from spent petrochemical catalysts to prepare them for pyrometallurgical recovery of Ni, Mo and V. Scientific Reports, 15, 8837. https://doi.org/10.1038/s41598-025-91247-x

Martín Treceño, S., Allanore, A., Bishop, C. M., Marshall, A. T., & Watson, M. (2021). Implications of direct use of slag from ironmaking processes as molten oxide electrolyte. JOM, 73(6), 1899–1908. https://doi.org/10.1007/s11837-021-04681-3

Ma, S., Li, Q., Peng, J., Jiang, Y., & Zou, Z. (2024). Large-scale dispersed phase-resolved direct numerical simulation (LDPR-DNS) of mechanically stirred reactors: Understanding the dispersion mechanism of multiphase flow and qualifying the droplets produced. Powder Technology, 439, Article 119707. https://doi.org/10.1016/j.powtec.2024.119707

Matsushita, T., Belov, I., Siafakas, D., Jarfors, A. E. W., & Watanabe, M. (2021). Interfacial phenomena between molten iron and molten slag–Effect of nitrogen on the Marangoni convection. Journal of Materials Science, 56, 7811–7822. https://doi.org/10.1007/s10853-020-05730-z

McGuan, R., Candler, R., & Kavehpour, H. P. (2022). The dynamics of bouncing, partially coalescing, liquid metal droplets in a viscous medium. Journal of Fluid Mechanics, 933, A29. https://doi.org/10.1017/jfm.2021.1090

Mendoza, S., Garlick, C., Singh, T., Nusheh, M., Yin, B. H., Honeyands, T., & Bumby, C. W. (2026). Melting behavior of hydrogen-reduced vanadium-bearing titanomagnetite ironsand pellets in a laboratory-scale electrode smelter. Journal of Sustainable Metallurgy, 12(2), 1176–1188. https://doi.org/10.1007/s40831-025-01389-5

Milani, V., & Timelli, G. (2023). Solid salt fluxes for molten aluminum processing—A review. Metals, 13(5), Article 832. https://doi.org/10.3390/met13050832

JIRRS
Journal International Review of Research Studies

Received: 19/09/2026 - **Accepted:** 26/10/2026
Vol: 01.07
DOI: 10.66104/p3c1fk38
Pages: 1-33

Milani, V., Vallejo-Olivares, A., Tranell, G., & Timelli, G. (2023). Influence of cryolite content on the thermal properties and coalescence efficiency of NaCl–KCl salt flux. In S. Broek (Ed.), Light Metals 2023 (pp. 928–935). Springer. https://doi.org/10.1007/978-3-031-22532-1_123

Minami, T., Katoh, K., Wakimoto, T., Ueda, Y., & Iguchi, M. (2023). Dynamic behavior of a metal droplet in contact with slag–metal interface. Journal of the Japanese Society for Experimental Mechanics, 23(1), 56–63. https://doi.org/10.11395/jjsem.23.56

Mirjalili, S., & Chan, W. H. R. (2021). Linear stability of a thin fluid film interacting with its surrounding bulk fluid. Physics of Fluids, 33(7), Article 072104. https://doi.org/10.1063/5.0056855

Mitas, B., Visuri, V.-V., & Schenk, J. (2022). Mathematical modeling of the ejected droplet size distribution in the vicinity of a gas–liquid impingement zone. Metallurgical and Materials Transactions B, 53(5), 3083–3094. https://doi.org/10.1007/s11663-022-02588-1

Mitas, B., Visuri, V.-V., & Schenk, J. (2023). Modeling the residence time of metal droplets in slag during BOF steelmaking. Metallurgical and Materials Transactions B, 54(4), 1938–1953. https://doi.org/10.1007/s11663-023-02808-2

Mongoljiibuu, S.-O., Lastam, J., Ditscherlein, R., Ebert, D., Müller, M., & Peuker, U. A. (2025). Chromium in slag from SOEL interconnects remelting: Characterization and recycling potential. Minerals, 15(9), Article 904. https://doi.org/10.3390/min15090904

Moosavi-Khoonsari, E., & Mostaghel, S. (2024). Thermodynamic assessment of tin-smelting from cassiterite concentrates. Canadian Metallurgical Quarterly, 63(3), 901–914. https://doi.org/10.1080/00084433.2023.2266209

Moosavi-Khoonsari, E., & Tripathi, N. (2024). Gold recovery from smelting copper sulfide concentrate. Processes, 12(12), Article 2795. https://doi.org/10.3390/pr12122795

Morales, R. D., Calderón-Hurtado, F. A., Chattopadhyay, K., & Guarneros Guarneros, S. J. (2020). Physical and mathematical modeling of flow structures of liquid steel in ladle stirring operations. Metallurgical and Materials Transactions B, 51(2), 628–648. https://doi.org/10.1007/s11663-019-01759-x

Nababan, D. C., Mukhlis, R., Durandet, Y., Prentice, L. H., & Rhamdhani, M. A. (2024a). Separation of Li and Co from $LiCoO_2$ cathode material through aluminothermic reduction: Investigation of the thermite reaction. Metallurgical and Materials Transactions B, 55(2), 905–924. https://doi.org/10.1007/s11663-024-03003-7

Nababan, D. C., Mukhlis, R., Durandet, Y., Prentice, L. H., & Rhamdhani, M. A. (2024b). Separation of Li and Co from $LiCoO_2$ cathode material through aluminothermic reduction: Thermodynamic calculations and experimental results. Metallurgical and Materials Transactions B, 55(1), 352–375. https://doi.org/10.1007/s11663-023-02962-7

JIRRS
Journal International Review of Research Studies

Received: 19/09/2026 - **Accepted:** 26/10/2026
Vol: 01.07
DOI: 10.66104/p3c1fk38
Pages: 1-33

Natsui, S., Tonya, K., Nogami, H., Kikuchi, T., Suzuki, R. O., Ohno, K.-I., Sukenaga, S., Kon, T., Ishihara, S., & Ueda, S. (2020). Numerical study of binary trickle flow of liquid iron and molten slag in coke bed by smoothed particle hydrodynamics. Processes, 8(2), 221. https://doi.org/10.3390/pr8020221

Park, W.-B., Park, J., Park, Y.-J., Park, S.-C., & Kang, Y.-B. (2026). Experimental investigation of hydrogen-based DRI melting behavior coupled with thermodynamic prediction for optimization of carburizing agents and flux blending conditions. Metallurgical and Materials Transactions B, 57, 5506–5525. https://doi.org/10.1007/s11663-026-04164-3

Pathak, A., Rana, M. S., Al-Sheeha, H., Navvamani, R., & Al-Sairafi, S. (2025). Sustainable extraction of valuable metals from petroleum spent hydroprocessing catalysts using a biodegradable lixiviant. Separation and Purification Technology, Article 128686. https://doi.org/10.1016/j.seppur.2024.128686

Pelusi, F., Guglietta, F., Sega, M., Aouane, O., & Harting, J. (2023). A sharp interface approach for wetting dynamics of coated droplets and soft particles. Physics of Fluids, 35(8), Article 082126. https://doi.org/10.1063/5.0160096

Pereira, A. C. (2026). From vanadium–titanium magnetite to Fe–C–V alloys: A critical review of vanadium-bearing pig iron production, vanadium partitioning, refining, and metallurgical applications. Journal International Review of Research Studies, 1(9), 1–48. https://doi.org/10.66104/qa1tk476

Pereira, A. C. (2026). Liquid-metal droplet coalescence in metallurgical slags: A critical review of interfacial phenomena, slag properties, hydrodynamics, kinetics, and metal recovery. International Journal of Research and Innovation in Social Science, 10(7), 15007–15036. https://doi.org/10.47772/IJRISS.2026.100701023

Pereira, A. C. (2026). Recovery and recycling of spent Ni–Mo–V catalysts: Technologies, environmental drivers and circular economy perspectives. IKR Journal of Multidisciplinary Studies, 2, 41–64. https://doi.org/10.5281/zenodo.18838023

Pereira, A. C. (2026). Scale-up in mineral processing: From mechanism preservation to flowsheet-scale transferability—A critical review and the MINESCALE framework. Journal of Advanced Multidisciplinary Studies, 1(III), 661–694. https://doi.org/10.68050/JAMS.2026.800

Pereira, A. C. (2026). Slag composition control indices in high-temperature metallurgy: A critical review of viscosity, conductivity, corrosion, and refractory wear. Journal International Review of Research Studies, 1(4). https://doi.org/10.66104/7x5etg23

Philipson, H. G. R., Wallin, M., & Einarsrud, K. E. (2024). Investigation of liquid–liquid reaction phenomena of aluminum in calcium silicate slag. Materials, 17(7), Article 1466. https://doi.org/10.3390/ma17071466

Qian, L., He, W., Liu, J., Zhu, C., Zhou, F., Ding, H., & Lin, J. (2023). Experimental investigation of the sedimentation behavior of metal droplets in liquid–liquid systems. Physics of Fluids, 35(2), 023304. https://doi.org/10.1063/5.0135636

JIRRS
Journal International Review of Research Studies

Received: 19/09/2026 - **Accepted:** 26/10/2026
Vol: 01.07
DOI: 10.66104/p3c1fk38
Pages: 1-33

Rämä, M., Klemettinen, L., Rinne, M., Taskinen, P., Michallik, R. M., Salminen, J., & Jokilaakso, A. (2023). Processing of a zinc leach residue by a non-fossil reductant. ACS Omega, 8(24), 21450–21463. https://doi.org/10.1021/acsomega.3c00250

Romero, J. L., Recksiek, V., Debastiani, R., Hossain, M. N., Blenau, L., Charitos, A., Väisänen, A. O., & Patil, A. B. (2026). Pyrometallurgical valorization of Waelz, fayalite, and Linz–Donawitz slag mixtures. Scientific Reports, 16, Article 9539. https://doi.org/10.1038/s41598-026-44763-3

Ruismäki, R., Dańczak, A., Klemettinen, L., Taskinen, P., Lindberg, D., & Jokilaakso, A. (2020). Integrated battery scrap recycling and nickel slag cleaning with methane reduction. Minerals, 10(5), Article 435. https://doi.org/10.3390/min10050435

Schrama, F. N. H., Beunder, E. M., Panda, S. K., Visser, H.-J., Moosavi-Khoonsari, E., Sietsma, J., Boom, R., & Yang, Y. (2021). Optimal hot metal desulphurisation slag considering iron loss and sulphur removal capacity part I: Fundamentals. Ironmaking & Steelmaking, 48(1), 1–13. https://doi.org/10.1080/03019233.2021.1882647

Schubert, C., Eickhoff, M., & Pfeifer, H. (2022). Numerical simulations of the molten metal droplet formation in the electroslag remelting process with a rotating electrode. Steel Research International, 93(12), 2100765. https://doi.org/10.1002/srin.202100765

Shimasaki, S., Ueda, S., Saito, N., & Katoh, K. (2024). Settling of particle in foaming slag. ISIJ International, 64(15), 2195–2202. https://doi.org/10.2355/isijinternational.ISIJINT-2024-274

Shi, Z., Ding, Y., Ren, J., He, X., Zhao, B., Zhong, J., Zhu, Y., Wang, B., & Zhang, S. (2024). Oxidation leaching of NiMoV alloy enriched from spent hydrogenation catalysts and solvent extraction of Mo and V. Journal of Environmental Chemical Engineering, 12(1), 111714. https://doi.org/10.1016/j.jece.2023.111714

Shi, Z.-S., Ding, Y.-J., Yin, X.-P., Liu, B., Shen, H.-L., Wu, B.-Y., Zhao, B.-H., Han, F.-L., Ekberg, C., & Zhang, S.-G. (2023). Enrichment of Ni–Mo–V via pyrometallurgical reduction from spent hydrogenation catalysts and the multi-reaction mechanism. Rare Metals, 42(8), 2700–2712. https://doi.org/10.1007/s12598-023-02278-0

Silva, A. M. B., Oliveira, M. A., Peixoto, J. J. M., & da Silva, C. A. (2021). Slag–steel emulsification on a modified RH degasser. Metallurgical and Materials Transactions B, 52(4), 2111–2125. https://doi.org/10.1007/s11663-021-02161-2

Spooner, S., Li, Z., & Sridhar, S. (2020). Hidden phenomena during transient reaction trajectories in liquid metals processing. Metallurgical and Materials Transactions B, 51(4), 1301–1314. https://doi.org/10.1007/s11663-020-01880-2

Sun, B., Guo, L., Wang, Z., Lan, X., & Guo, Z. (2024). Sustainable recycling of pure aluminum from waste chips under supergravity-enhanced separation: A cleaning process. Sustainable Materials and Technologies, 42, Article e01148. https://doi.org/10.1016/j.susmat.2024.e01148

JIRRS
Journal International Review of Research Studies

Received: 19/09/2026 - **Accepted:** 26/10/2026
Vol: 01.07
DOI: 10.66104/p3c1fk38
Pages: 1-33

Sun, B., Guo, L., Wang, Z., Lan, X., & Guo, Z. (2025). Direct collection and reuse of dispersed aluminum chips through salt flux and supergravity enrichment: Less salt consumption and circular economy. Journal of Cleaner Production, 521, Article 146230. https://doi.org/10.1016/j.jclepro.2025.146230

Sun, S., Yang, K., Liu, C., Tu, G., & Xiao, F. (2024). Recovery of nickel and preparation of ferronickel alloy from spent petroleum catalyst via cooperative smelting–vitrification process with coal fly ash. Environmental Technology, 45(11), 2108–2118. https://doi.org/10.1080/09593330.2021.2002421

Suzuki, M., Iwakura, K., Tsukaguchi, Y., & Mishima, K. (2024). Effect of fluoride ions in slag on the dynamic change of the interfacial tension between liquid iron and molten slag. ISIJ International, 64(15), 2217–2225. https://doi.org/10.2355/isijinternational.ISIJINT-2024-134

Suzuki, M., & Nakamoto, M. (2022). Effect of B_2O_3 addition to slag on the dynamic change behavior of interfacial tension between liquid iron and molten slag. ISIJ International, 62(7), 1334–1340. https://doi.org/10.2355/isijinternational.ISIJINT-2021-605

Tangstad, M., Olsen, J. E., Ringdalen, E., Ksiazek, M., Reynolds, Q., & Steenkamp, J. (2022). Conceptual tapping model of Mn-ferroalloy furnaces. JOM, 74(11), 3962–3970. https://doi.org/10.1007/s11837-022-05474-y

Tian, C., Gao, Y., Zhao, W., Ling, Z., Li, Z., Xie, H., & Mao, B. (2026). Recovery of valuable metals from spent HDS catalysts and comprehensive utilization of spent HDS. Separations, 13(8), 218. https://doi.org/10.3390/separations13080218

Tian, M., Wang, Q., Wang, S., Wan, X., Wang, Q., & Guo, X. (2024). Multiphase equilibrium relationships between copper matte and $CaO–Al_2O_3$-bearing iron silicate slags in combined smelting of WEEE and copper concentrates. Sustainability, 16(2), Article 890. https://doi.org/10.3390/su16020890

Tian, X., Guo, Z., Li, B., Zhu, D., Pan, J., Yang, C., Li, S., & Zhao, F. (2026). Green utilization of zinc smelting slag by hydrogen reduction: Role of MgO in metal separation and recovery. Process Safety and Environmental Protection, 212, Article 108918. https://doi.org/10.1016/j.psep.2026.108918

Tsebe, S. P., & Steenkamp, J. D. (2024). Development of an integrated process flowsheet to recover valuable metals from waste cathode ray tubes and printed circuit boards. Journal of Sustainable Metallurgy, 10(1), 224–240. https://doi.org/10.1007/s40831-023-00775-1

Vergote, O., Van den Bulck, A., Bellemans, I., & Verbeken, K. (2025). Rheological behavior of slag–melilite suspensions in pyrometallurgical secondary lead smelter systems. Journal of Rheology, 69(6), 973–989. https://doi.org/10.1122/8.0001033

JIRRS
Journal International Review of Research Studies

Received: 19/09/2026 - **Accepted:** 26/10/2026
Vol: 01.07
DOI: 10.66104/p3c1fk38
Pages: 1-33

Wang, G., Hui, H., Cui, Y., Li, X., Yang, S., Yang, Y., & He, Y. (2026). The interfacial adhesion behaviors of sedimentation zone in flash smelting based on DFT calculation (Part II)—The adhesion mechanisms of Fe_3O_4 with FeS, Ni_3S_2 and Cu_2S. Metallurgical and Materials Transactions B, 57(3), 1605–1619. https://doi.org/10.1007/s11663-026-03948-x

Wang, J., Fan, E., & Wu, Y. (2025). Numerical modeling of Marangoni flow between steel droplet and slag induced by concentration gradient. Canadian Metallurgical Quarterly. Advance online publication. https://doi.org/10.1080/00084433.2025.2580025

Wang, Q.-M., Huang, M.-X., Yan, S.-Y., Wang, S.-S., Tian, Q.-H., & Guo, X.-Y. (2023). Hydrodynamic simulation of metal droplet settlement in molten slag. Transactions of Nonferrous Metals Society of China, 33(4), 1244–1257. https://doi.org/10.1016/S1003-6326(23)66179-5

Wang, R., Zhang, B., Liu, C., & Jiang, M. (2025). Physical modeling of bottom-blown bubble penetration dynamics at slag/metal interface in metallurgical reactors. Colloids and Surfaces A: Physicochemical and Engineering Aspects, 727, Article 138296. https://doi.org/10.1016/j.colsurfa.2025.138296

Wang, Z., Gao, J., Lan, X., & Guo, Z. (2024). A green method to clean copper slag and rapidly recover copper resources via reduction-sulfurizing smelting and super-gravity separation at low temperature. Journal of Hazardous Materials, 468, 133834. https://doi.org/10.1016/j.jhazmat.2024.133834

Wang, Z., Gao, J., Lan, X., & Guo, Z. (2025). An eco-friendly approach for enhanced separation and efficient recovery of copper matte from molten copper smelting slag via supergravity. Process Safety and Environmental Protection, 202, 107707. https://doi.org/10.1016/j.psep.2025.107707

Wang, Z., Gao, J., Lan, X., & Guo, Z. (2023). Sustainable recovery of metallic Al and reuse of molten salt in Al dross: Salt flux erosion and super-gravity separation. Journal of Cleaner Production, 431, Article 139809. https://doi.org/10.1016/j.jclepro.2023.139809

Wang, Z., Gao, J., Lan, X., & Guo, Z. (2024). Joint utilization and harmless elimination of aluminum dross and refined magnesium slag to simultaneously recover metallic aluminum and fusing agent. Journal of Environmental Management, 366, Article 121680. https://doi.org/10.1016/j.jenvman.2024.121680

Wan, Z., Yang, S., & Wang, H. (2024). Multiphase stirring dynamics of gas–slag–matte in large-scale side-blown copper bath smelting process. Journal of Sustainable Metallurgy, 10(2), 992–1006. https://doi.org/10.1007/s40831-024-00841-2

Wei, G., Wang, H., Ju, J., Yang, Y., & Jiang, X. (2026). Kinetic model for vanadium extraction by CO_2–O_2 mixed injection based on interfacial reactions of emulsified droplets. Metallurgical and Materials Transactions B. Advance online publication. https://doi.org/10.1007/s11663-026-04188-9

JIRRS
Journal International Review of Research Studies

Received: 19/09/2026 - **Accepted:** 26/10/2026
Vol: 01.07
DOI: 10.66104/p3c1fk38
Pages: 1-33

Wu, C., Wang, J., Bai, J., Kong, L., Guo, Z., Li, H., Bai, Z., & Li, W. (2025). Study of the relationship between solid phase transformation and flow behavior transitions driven by carbothermal reaction in slag of BGL gasification. Energy, 340, Article 139263. https://doi.org/10.1016/j.energy.2025.139263

Wu, C., Wang, J., Bai, J., Kong, L., Guo, Z., Li, H., Bai, Z., & Li, W. (2026). Mechanistic insights into metallic iron-induced changes in viscosity, structure, and iron agglomeration of fixed-bed gasifier slag. Fuel, 424, Article 139397. https://doi.org/10.1016/j.fuel.2026.139397

Xhaferaj, N., & Ferella, F. (2022). Extraction and recovery of metals from spent HDS catalysts: Lab- and pilot-scale results of the overall process. Metals, 12(12), 2162. https://doi.org/10.3390/met12122162

Xiao, W., Yao, S., Zhou, S., Wei, Y., Li, B., & Wang, H. (2022). Evolution of the structure and viscosity of copper slag during metallization-reduction. Journal of Alloys and Compounds, 903, 163751. https://doi.org/10.1016/j.jallcom.2022.163751

Xin, J., Wang, N., Chen, M., & Chen, C. (2020). Slag–metal separation and reduction behaviors of vanadium-bearing titanomagnetite metalized pellets. ISIJ International, 60(5), 823–831. https://doi.org/10.2355/isijinternational.ISIJINT-2019-529

Xin, Z.-C., Lin, W.-H., Zhang, J.-S., Peng, K.-X., & Liu, Q. (2025). Modeling the decarburization of expansion droplets based on the solid phase ratio of slag and data fitting during BOF steelmaking process. Scientific Reports, 15, Article 16346. https://doi.org/10.1038/s41598-025-01424-1

Xu, X., Zhou, S., Li, B., Wei, Y., & Wang, H. (2025). Investigation interfacial wetting behavior of copper matte/slag/Fe_3O_4 enriched intermediate layer during high temperature smelting. Metallurgical and Materials Transactions B, 56(1), 449–471. https://doi.org/10.1007/s11663-024-03370-1

Yang, M., Yan, Z., Li, Z., Lv, X., & Bai, C. (2025). Modelling the dissolutive wetting of slag-oxide system at high temperatures. Metallurgical and Materials Transactions B, 56, 1573–1587. https://doi.org/10.1007/s11663-024-03429-z

Zhang, D., Liu, Y., Hu, Q., Ke, X., Yuan, S., Liu, S., Ji, X., & Hu, J. (2020). Sustainable recovery of nickel, molybdenum, and vanadium from spent hydroprocessing catalysts by an integrated selective route. Journal of Cleaner Production, 252, 119763. https://doi.org/10.1016/j.jclepro.2019.119763

Zhang, J., Zhao, B., & Yan, B. (2023). Analysis of emulsification behavior and kinetics of reaction between high-Al molten steel and CaO–SiO_2 flux. Metallurgical and Materials Transactions B, 54(3), 981–988. https://doi.org/10.1007/s11663-023-02749-w

Zhang, L., & Chen, M. (2023). Recovery of valuable metals and production of Fe–V crude alloy from vanadium-enriched slag using aluminum dross as a reductant. JOM, 75(4), 1180–1191. https://doi.org/10.1007/s11837-022-05561-0

JIRRS
Journal International Review of Research Studies

Received: 19/09/2026 - **Accepted:** 26/10/2026
Vol: 01.07
DOI: 10.66104/p3c1fk38
Pages: 1-33

Zhang, P., Zhang, H., Deng, G., Li, D., Hu, J., Tan, C., Yu, Y., Fan, R., & Wang, H. (2026). Turbulence modulation via internal baffles for intensified slag–matte separation in gas-stirred reactors. Journal of Sustainable Metallurgy, 12(3), 3181–3199. https://doi.org/10.1007/s40831-026-01503-1

Zhao, B., Zhang, J., & Yan, B. (2022). Interfacial phenomena and reaction kinetics between high Al molten steel and CaO–SiO_2-type flux. Metals, 12(3), Article 391. https://doi.org/10.3390/met12030391

Zoraga, M. (2024). Metal recovery from spent Ni-Mo-V hydrodesulphurisation catalyst in oxalic acid media by mechanochemical treatment. Canadian Metallurgical Quarterly, 63(3), 882–891. https://doi.org/10.1080/00084433.2023.2221579